# Bismuth oxide nanostructure supported on Cu foam as efficient electrocatalyst toward carbon dioxide electroreduction

Ismail Husein[1] · Jihad M. Hadi[2] · A. Surendar[3] · Natalya N. Gryzunova[4] · Rezeda G. Khairullina[5] · Dmitry O. Bokov[6] · Huynh Tan Hoi[7]

## Abstract

Bismuth-based catalysts have emerged as promising materials for efficient electrochemical reduction of carbon dioxide due to their unique electronic and catalytic properties. In this work, we present a new type of hybrid nanomaterials compositing of partially reduced oxide Bi particle into metallic Bi anchored on 3D network of Cu foam as a high-performance catalyst for electrochemical $CO_2$ conversion to formate. $CO_2$ electroreduction in neutral condition with high durability has remained challenging. One of the main stability problems of Bi catalysts is their susceptibility to surface oxidation, which can cause the deactivation of the catalyst during electrochemical reactions. Under proper bismuth growth control, herein, our strategy on preparing Bi/Cu foam catalyst demonstrated high $CO_2$ electrochemical reduction performance with formate faradaic efficiency of more than 90% with a great stability of 50-h operation at an applied current density of 50 mA cm$^{-2}$ in a neutral environment. The catalyst fine nanostructures resulted in high available active sites and high conductivity of substrate have resulted in its great durability and selectivity.

**Keywords** $CO_2$ electroreduction · Bismuth nanostructures · Galvanic exchange · Cu/Bi interaction

## Introduction

It goes without saying that the $CO_2$ greenhouse gas release into atmosphere has resulted several serious human-related health and environmental-related problems, such as earth temperature rise, sea level rise, and so on [1, 2]. Thereby, there is great demands and also necessity to reduce the $CO_2$ gas emission or its concentration from the air to ameliorate the destructive effects and produce value added chemicals as energy resources to overcome energy crisis [3, 4]. So far, $CO_2$ electroreduction through electrochemical reactions and carbon capture following with sequestration (CCS) located among the most widespread dealings in lowering $CO_2$ releases, which finally allow $CO_2$ to be reduced from air and convert into more useful fuels such as methanol, formic acid, ethylene and so on, and moreover carbon capture would result in $CO_2$ to be concentrated and accumulated in both water-soluble and insoluble carbonates compounds [5, 6]. Yet, the large-scale operation of $CO_2$ electroreduction and CCS technology is restricted by their high-level energy utilization and high-priced industrial expenses. On the other hand, $CO_2$ conversion, capture and utilization attained great focus owing to its outstanding behavior as sustainable and influential alternative to conventional energy sources [1, 7]. It would be worthy to note that $CO_2$ electrocatalytic reduction ($CO_2$ER) has the capability of converting $CO_2$ into single or multi-carbon products which are good sources of fuels (e.g., formate

✉ Ismail Husein
husein_ismail@uinsu.ac.id

1 Department of Mathematics, Universitas Islam Negeri Sumatera Utara, Medan, Indonesia

2 Department of Medical Laboratory of Science, College of Health Sciences, University of Human Development, Kurdistan Regional Government, Sulaimani 46001, Iraq

3 Department of Pharmacology, Saveetha Dental College and Hospital, Saveetha Institute of Medical and Technical Sciences, Chennai, India

4 Department of Nanotechnology, Materials Science and Mechanics, Togliatti State University, Tolyatti, Russia

5 Kazan Federal University, Kazan, Russia

6 Institute of Pharmacy, Sechenov First Moscow State Medical University, 8 Trubetskaya St., Bldg. 2, Moscow 119991, Russian Federation

7 Language Department, FPT University, Hanoi, Vietnam

(HCOOH), carbon monoxide (CO), methane ($CH_4$) and ethylene ($C_2H_4$) and ethanol ($CH_3CH_2OH$)) in a wide range of conditions (in term of solution pH ranges), and it would be easily merged together with other renewable energy resources such as wind, tidal energy, and solar radiation, offers an operative plan for ideal employment of carbon sources and release of greenhouse gases [8, 9]. Nevertheless, $CO_2ER$ yet deal with numerous challenges, like as high-energy requirement (as overpotential or full-cell potential), low faradaic efficiency for a specific product, and low $CO_2$ conversion rate (applied current density) due to Hydrogen evolution reaction as competitive reaction [9, 10].

It is well-documented that applying structural and chemical modifications to the electrocatalyst is one of the most effective ways to improve the catalytic performance toward $CO_2ER$ [9, 11]. Up to date, the most commonly utilized materials are transition-metal-based materials (e.g., metals, metal alloys, metal carbides and metal oxides) which are comparable or even in some cases better that stat-of—the-art materials for electrocatalytic activity. But these materials have encountered some problems which are related to their inadequate conductivity and stability (chemical and corrosion resistance), poor electrocatalytic productivity and selectivity toward specific product, and some these materials are expensive at high purity, which is important to the $CO_2ER$ process. Thus, development of cost-effective electrocatalyst with good durability under practical operation of $CO_2ER$ and at the same time obtaining high selectivity as well as electrocatalytic performance would be highly significant to this field. With being said that good potentials of Bismuth-nanosheets (Bi-NSs) initiate from the exclusive structure of Bi-NSs has been found to be an imposing aspect for electrocatalytic reduction of $CO_2$. Unfortunately, Bi-based structures possess low electron conductivity, high affinity to oxidization and difficulty in the synthesize of 2-dimensional layers of Bi structure through employing conventional routes. Therefore, these drawbacks have hindered its wide utilization as industrial applications. Thereby, there is a serious demand to explore simple and real-operational methods for the preparation of Bi-based catalyst toward $CO_2ER$.

One of the main problems of Bi catalysts is their low operational stability under applied current densities. This is due to their susceptibility to surface oxidation, which can cause the deactivation of the catalyst during electrochemical reactions. The oxidation of the Bi surface leads to the formation of bismuth oxide ($Bi_2O_3$) or bismuth oxyhydroxide (BiOOH) species that inhibit the catalytic activity of Bi for $CO_2$ reduction.

Another stability issue of Bi catalysts is their tendency to undergo structural changes during the electroreduction process, which can result in the formation of new surface phases that exhibit different catalytic properties. These structural changes can also cause the aggregation or detachment of Bi particles from the electrode surface, leading to a decrease in catalytic activity and stability.

Addressing these stability issues of Bi catalysts is crucial for their practical applications in $CO_2$ electroreduction. Researchers are currently investigating various strategies such as surface modification, alloying, and optimization of the reaction conditions to enhance the stability of Bi catalysts for $CO_2$ reduction.

To follow up the abovementioned issues, herein, we put forward a step to create a Bi-based catalyst through using easy and reproducible galvanic exchange reaction and optimize it. The reaction that occurs in galvanic process is a redox type as soon as an element expose to another one and possesses small reduction potential than the one is in contact with inside an organic solution [12]. It is clear that the oxidation–reduction potential differences result in the impulsive metal oxidation and dissolution in solution, and concurrently, the metal ions deposition and reduction from solution will happen. Galvanic exchange reactions have been extensively utilized for the fabrication of porosity structures from gold, palladium and even in some cases platinum-based structures via utilizing a sacrificial metal as templates [12]. This concept can be expanded to further metals but has been poorly investigated outside of noble metals. As a proof of stated concept, we show that the galvanic exchange between Bi ions and copper substrate can produce a thickly and precipitously aligned nanolayers on Cu foam as platform. In this regard the produced Bi-Cu material with well-prepared nanostructures employed as the electrocatalyst for $CO_2ER$ to formate in neutral condition. It shows superior Faradaic efficiency of > 90% for formate at high conversion rate of 50 mA cm$^{-2}$ and long-term durability of about 50 h.

# Experimental section

## Catalyst preparation

Generally, the Bi nanosheets were grown on Cu foam support, 0.2 M of $Bi(NO_3)_3$ dispersed in 25 dimethylformamide (DMF). Before growing process, the Cu foam was cut into pieces and washed with 1 M HCl, and rinsed with acetone and then with DI water. Afterward, the prepared Cu substrate was put into the prepared above solution for three different times, 24, 48, and 72 h. The samples were named as Cu/Bi$_{24}$, Cu/Bi$_{48}$, and Cu/Bi$_{72}$ based on their growth time. Afterward, the prepared samples were treated under atmosphere condition at 100 °C for 10 h. The synthesized samples were utilized as cathodic electrodes to convert $CO_2$ into valuable formate.

## Material characterization

For crystalline structure evaluations, X-ray diffraction (XRD) pattern was employed. The size and morphological features of the prepared samples were examined on a scanning electron microscope (SEM, Zeiss, Germany). The X-ray photoelectron spectroscopy (XPS) measurements were conducted using a VG Escalab 220i-XL spectrometer with a Polychromatic Al $K_\alpha$ radiation (1486.6 eV). The samples were analyzed in an area of $5 \times 5$ mm$^2$ at a pressure of approximately $1*10^{-9}$ mbar in the analysis chamber. During the scan survey, spectra were taken with a constant pass energy of 100 eV and a step size of 1 eV. Additionally, high-resolution spectra of Bi 4f core levels were recorded with a constant pass energy of 20 eV and a step size of 0.1 eV. The take-off angle, which is the angle between the surface normal and the detection direction, was $\theta = 0°$ for all measurements. To calibrate the binding energy scale, the $C_{1s}$ peak at 284.6 eV was used as a reference point due to hydrocarbon contamination.

All the spectra collected were analyzed using the CasaXPS software (Casa Softw. Ltd., 2005), with the nonlinear Shirley-type background method applied to the Bi 4f core peaks. This analytical method is a popular and effective approach for analyzing core-level XPS data.

## Electrochemical measurements

Electrochemical analyses were recorded in a two-compartment cell system (normally known as H-cell) utilizing conventional three-electrode system. In this three-electrode system, we have used Ag/AgCl (3 M KCl) as reference electrode positioned in cathode side, a Cu foam as counter electrode in anode side. And for the working electrode part, the prepared electrode samples were utilized and put them in cathode compartment. The two sides of the H-cell system (anode and cathode) were separated from each other by using bipolar membrane (BPM) and each part filled with 50 mL solution, the cathode side filled with 0.5 M KHCO$_3$ saturated with CO$_2$ gas and the anode part filled with 0.5 M KOH. The cathode was continuously purged with CO$_2$ gas with a flowing rate of 12 sccm. Linear sweep voltammetry was applied at a scan rate of 5 mV s$^{-1}$. Electrochemical impedance spectroscopy was conducted at frequency range of 0.1–10$^5$ Hz with a potential amplitude of 10 mV. To obtain EIS results, we took two different conditions at open-circuit potential (OCP) and at applied potentials (different potentials were used which is mentioned in their section). The EIS test was conducted in 1 M KOH as electrolyte. The gas products were measured by using gas chromatography (Aligent 7890B model). The faradaic efficiency of the gaseous products was calculated through utilizing GC results. The peak area related to each gas products (H$_2$ and CO) was obtained from GC, and then employed Eq. 1 to calculate the final gas product faradaic efficiency:

$$FE = \frac{S_x \times \text{gas flow}}{329.6 \times J_{applied}} \times 100 \qquad (1)$$

where $S_x$ stands for the calculated peak area for each of the gas products, gas flow is the CO$_2$ gas feed rate in s.c.c.m., and $J_{applied}$ is the total applied current. And liquid product (here is formate) was evaluated through using nmr instrument.

## Results and discussion

In this work, the galvanic exchanged (GE) process is done by immersing the Cu foam into 0.2 M dimethylformamide (DMF) solution, which to do this, no surfactant or ligands have utilized, as described in the details in the "Experimental section". Since the reduction potential of Bi (0.31 V vs. RHE) is smaller than Cu reduction potential (0.34 V vs. RHE), through further addition of Bi concentration into the solution, the GE process can happen. In fact, due to the different ion's concentration inside the solution, the reduction reaction will be changed to have the following reaction: $2Bi^{3+} + 3Cu \rightarrow 2Bi + 3Cu^{2+}$. It should be noted that the mentioned reaction is not spontaneous through considering the standard state.

It should be noted that the Nernst equation considers the concentration of the reactants and products and allows us to measure the actual cell potential, which determines the spontaneity of the reaction.

The Nernst equation is:

$$E = E° - (RT/nF) * ln(Q)$$

where in the above equation, $E$ stands for the cell potential, $E°$ shows the standard cell potential, $R$ shows the gas constant, $T$ also shows the temperature in K, $n$ shows the number of electrons transferred, $F$ shows Faraday's constant, and $Q$ shows the reaction quotient [13, 14].

If we consider the Bi reduction case, it can be written as a half-reaction as follows:

$$Bi^{3+} + 3e^- \rightarrow Bi_{(s)}$$
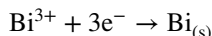
The standard reduction potential for this reaction is $-0.279$ V. However, the actual cell potential depends on the concentrations of Bi$^{3+}$ and Bi in the reaction mixture. If the concentration of Bi$^{3+}$ is high enough, the reaction can occur spontaneously [14–16].

Therefore, considering the abovementioned discussion on Bi reduction, we can say that when a blank Cu substrate soaks into DMF solution containing 0.2 M Bi ions

and without any additional Cu ions, the equilibrium will be shifted as a result of Nernstian cooperation in this regard. Therefore, the mentioned reaction is possible, which finally results in slow Cu ion degradation and replacement with

Bi ions on the platform and further growth leads to dense nanosheets on Cu substrate. Figure 1a shows the smooth surface of the Cu foam without any sharp edges on top of it. However, after galvanic exchange of Bi on Cu, the SEM
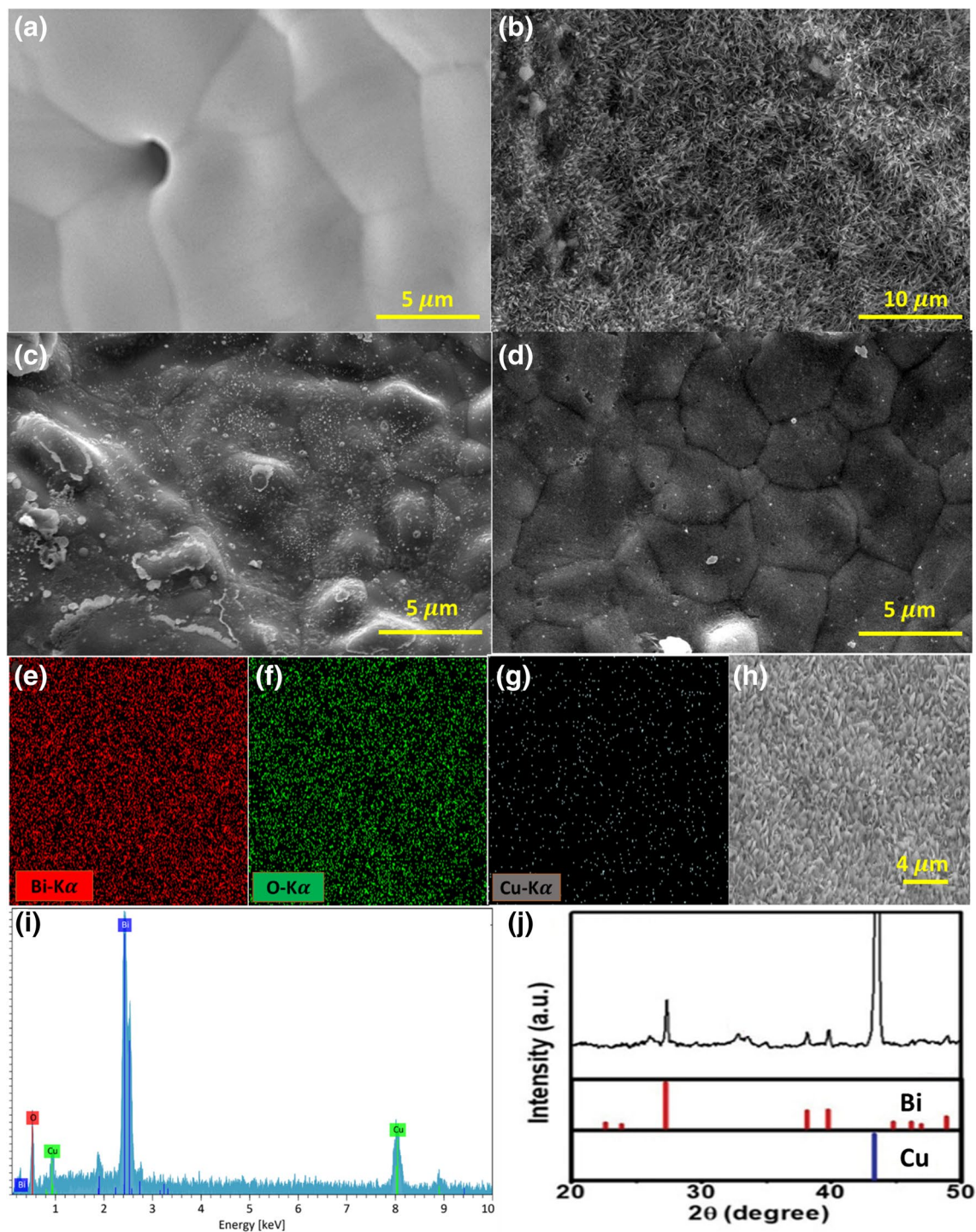


**Fig. 1** The SEM images of **a** bare Cu foam surface, **b** optimized Bi growth on Cu support, **c, d** 24-h and 72-h Bi growth on Cu foam, respectively, **e–h** mapping result of the optimized Bi growth on Cu, **i** the EDX profile for optimized sample, and **j** the XRD profile for the optimized Bi sample

images in Fig. 1 (b-d) show the successful growth of Bi on Cu substrate. As can be seen from Fig. 1b, the optimized Bi layer is made of many sharp corners and edges on Bi nanowire-type morphology, in which these sharp sites would accumulate charge intensity at local area and offer numerous active sites with high surface energy that can promote the catalytic reaction. The morphology of optimized catalyst demonstrates nanowires in nanometer ranges with many defects and porosity, which is different than the other two catalysts (Fig. 1 b-d). These surface properties of the prepared electrode have efficiently contributed to the enhancement of electrocatalytic reaction by providing higher accessible surface area and high electrical intensity, and high crystallinity of the structure. However, the more Bi growth time increased, the more surface morphology became coarse, which also has blocked all those sharp sites which could be beneficial for catalytic activity (Fig. 1c). And when the growth time was not enough (24 h), the Bi deposition was incomplete, in which there are traces of uncovered Cu surface (Fig. 1d). The mapping and EDX analysis also confirm the presence of Bi on Cu surface (Fig. 1i). And from mapping images, it can be seen that the Bi is almost uniformly grown on Cu surface (Fig. 1e-h). The XRD profile is shown in Fig. 1j for the optimized electrode. The obtained pattern is in good agreement with the reported works in literature [17, 18]. The observed peaks are related to the metallic Bi on Cu foam which has gathered after the deposition. The high intense peak at around 44° is related to Cu crystalline structure which is contributed from substrate [19]. Small peaks are also observed which are for partially oxidized Bi during or maybe after GE process. It seems that the XRD and SEM results are in good agreement. XPS is a highly useful technique for identifying the chemical composition of materials and their surfaces. It can provide information on the chemical states of elements in a sample, their chemical bonding environment, and their depth distribution. XPS is used extensively in materials science, chemistry, physics, and many other fields. As can be seen from Fig. S1, the XPS spectrum of Bi oxide typically shows two major peaks, one at a binding energy of approximately 159 eV corresponding to the Bi 4f7/2 core level and the other at around 164 eV corresponding to the Bi 4f5/2 core level. These peaks can be attributed to $Bi^{3+}$ and $Bi^{5+}$ ions in the oxide, respectively [20–22].

## Electrochemical $CO_2$ reduction

Figure 2a demonstrates LSV plots for the optimized electrode which has conducted in 0.5 M $KHCO_3$ electrolyte under both $CO_2$ saturated and $N_2$ saturated bicarbonate solution. The literature has established that bismuth (Bi) exhibits high activity for $CO_2$ electroreduction but lower activity for the hydrogen evolution reaction (HER), as supported by our LSV results. Therefore, the Bi-based sample displayed superior activity for $CO_2$ electrocatalysis compared to the HER reaction [20, 23]. Figure 2b demonstrates that the growth of Bi on Cu foam resulted in a higher current response with a smaller overpotential compared to blank Cu foam during $CO_2$ conversion under $CO_2$ gas flow. This higher electrocatalytic performance can be ascribed to the presence of many structural defects with sharp edges and corner sites, accumulated local intensities of electric field in the vicinity of those defects or edges or structural displacements, and therefore leads to higher performance toward $CO_2ER$ through increasing potassium ion concentration on catalyst surface [24]. In addition to that, the LSV results for HER in $N_2$ saturated condition, the overpotential required to reach a specific current density, and also the onset potential to initiate HER process were more negative than $CO_2$ saturated condition, which means that the optimized Bi-Cu sample performed better for $CO_2ER$ and suppressed the HER process. And it can inhibit HER process and do better catalytic activity toward $CO_2ER$ with lower overpotential and onset potential. Moreover, the optimized sample (Bi-Cu) demonstrated better performance than blank Cu sample.

The as-prepared catalysts were used to investigate their catalytic activity toward $CO_2ER$ for formate production at different applied potentials (ranging from $-1$ to $-2$ V (vs. Ag/AgCl)) in 0.5 M $KHCO_3$ as catholyte and 0.5 M KOH as anolyte. For the anode side, an Ni foam was utilized as it is highly stable in basic condition. The selectivity results for the prepared samples are shown in Fig. 2c in which the products have evaluated through well-known methods (gas chromatography for gas products, and NMR for liquid products). Most commonly, a lower gas product of less than 15% was observed for the $Cu/Bi_{48}$ sample in the tested potential ranges. Through nmr evaluation, we have observed that formate is the most omnipotent product of the $CO_2ER$ process and detected in all of the tested potential ranges. As can be seen from Fig. 2c, through increasing the applied potential, the FE for formate is increasing and reached to its highest selectivity at applied potential of $-1.6$ to $-1.8$ V (vs. Ag/AgCl) with high FE of around 90% before it begins to drop as a result of the possible HER competing reaction. It seems that at lower applied potentials, the HER is highly likely to happen on catalyst surface due to the onset potential for $CO_2RR$, while when the applied potential increased, the FE for formate enhanced significantly. And when the applied potential raised to $-2$ V, the FE for formate is also dropped. This could be due to the fact that the $CO_2$ concentration in solution is limited (0.34 mM) so the gas feed is the controlling issue at higher applied potential. The partial current density was evaluated and is shown in Fig. 2d. Figure 2d shows the partial current density of formate at different applied potentials for prepared samples. As can be seen from Fig. 2d, the partial current density for optimized
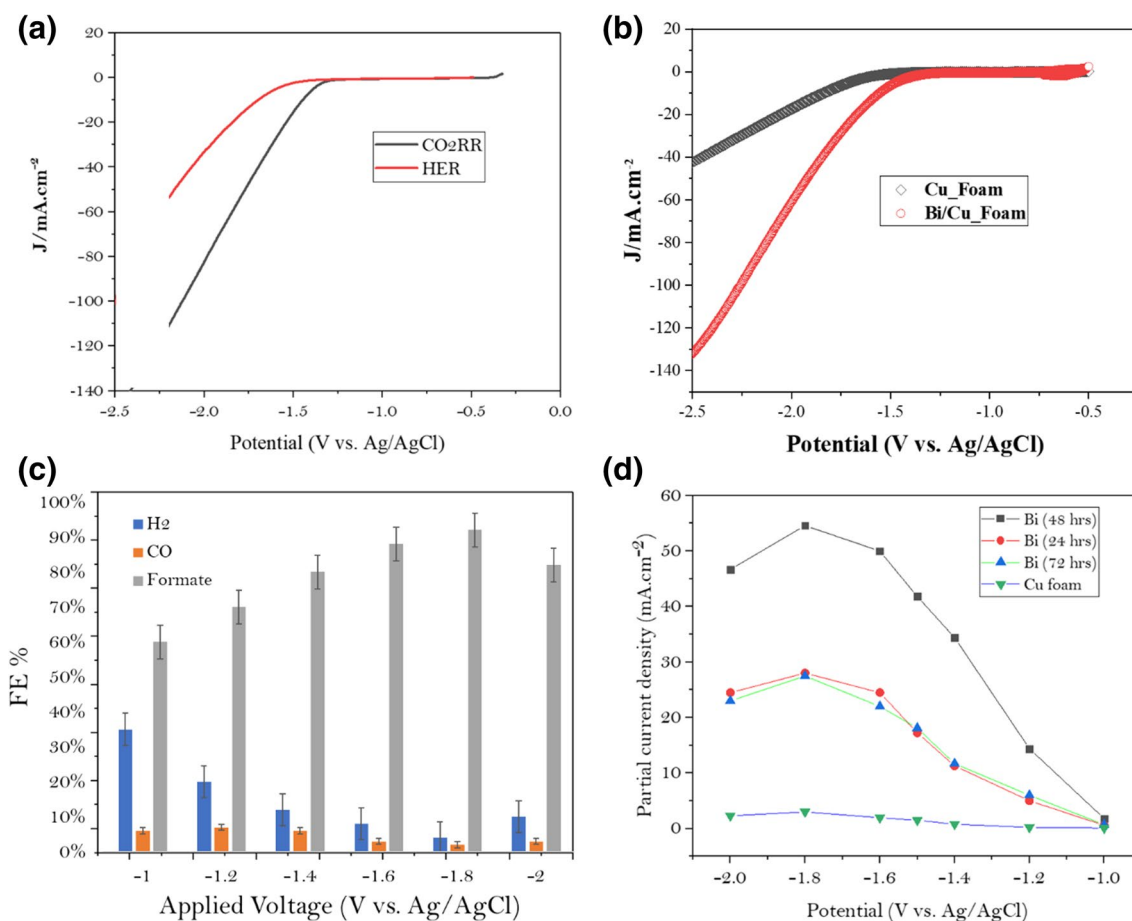
**Fig. 2** **a** The LSV curves for the optimized Bi sample, black line shows $CO_2RR$, red line shows HER, **b** LSV curves for bare Cu foam and Bi growth Cu foam under $CO_2$ gas flow into electrolyte, **c** selec- tivity related to the applied potentials, and **d** partial current densities for formate selectivity for each at relevant potentials for all of the samples

Bi-Cu sample delivers high current density of 54.6 mA cm$^{-2}$ at − 1.8 V (vs. Ag/AgCl), but it takes off in terms of selectiv- ity at − 1.8 V, whereas for the other Bi-based electrode, the partial current reached ≈ 28 mA cm$^{-2}$ and for the other one, it reached to ≈ 27 mA cm$^{-2}$, but for the blank Cu foam, the partial current density for formate reached to ≈ 3 mA cm$^{-2}$. It should be highlighted that the obtained partial current den- sity for the prepared samples in the H-cell system is highly impressive for $CO_2ER$ process. It should be noted that the importance of well-shaped surface structure of the optimized Bi deposition time and also the higher active sites of Cu/ $Bi_{48}$ than bare Cu foam has resulted in better $CO_2ER$ perfor- mance. And although the bare Cu foam can also be used as electrocatalytic activity, the copper foam is thickly covered up with Bi nano-needles (as can be seen from SEM images), and thus, its influence on $CO_2ER$ here can be considered negligible, which means the high performance is associated with Bi nanostructures solely. Moreover, there are abundant pores between neighboring nanosheets that form passages for the facile mass transport and diffusion in and out of the

nanosheets which has demonstrated higher partial current and better selectivity to formate [25, 26]. Also the selectivity of the different samples ($Cu/Bi_{24}$, $Cu/Bi_{48}$, $Cu/Bi_{72}$, and Cu bare) for gas products and formate is compared in Fig. S2, and all experiments were conducted under a constant poten- tial of − 1.8 V (vs. RHE). It is clear that the $Cu/Bi_{48}$ possess highest selectivity to formate due to its optimized condition with better exposer of active sites to electroreduction of $CO_2$.

Electrochemical studies of the prepared samples are shown in Fig. 3. To further investigate selectivity changes, EIS analysis was employed at different conditions, includ- ing $CO_2$ gas flow inside catholyte and $N_2$ gas flow inside the catholyte for HER process. In Fig. 3(a), Nyquist curves at open-circuit potential (OCP) are shown for both $N_2$ and $CO_2$ gas flow conditions. We have conducted the EIS test for $Cu/Bi_{48}$ sample. Under $N_2$ flow, the electrode demon- strated resistance behavior, whereas under $CO_2$ gas flow, the catalyst demonstrated Warburg behavior, indicated by an angle of almost 45°. These results suggest that when $CO_2$ is saturated, the selectivity for $CO_2$ conversion suppresses the

**Fig. 3** **a** Nyquist plots at **a** OCP condition under $N_2$ gas flow and $CO_2$ gas flow, **b** under HER and $CO_2RR$, **c** different voltages for $CO_2RR$, and **d** different current responses for $CO_2RR$
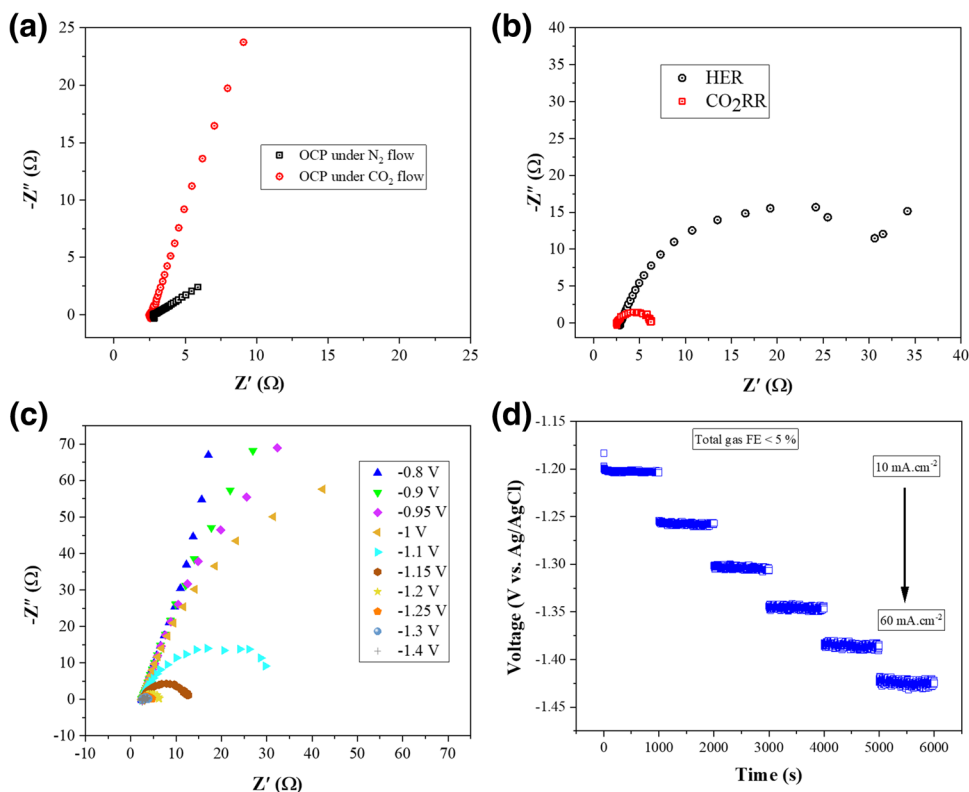


hydrogen evolution reaction (HER) process and enhances the activity for $CO_2$ conversion. Furthermore, a sharp angle at low frequencies was observed for the $CO_2$-saturated solution, indicating a high diffusion capability for $CO_2$ electroreduction. This study was also conducted at higher overpotentials for both HER and $CO_2$ reduction reactions, as shown in Fig. 3(b). The $CO_2$ reduction reaction showed a smaller charge transfer resistance (4.5 $\Omega$ $cm^2$) than that for HER (34.5 $\Omega$ $cm^2$). In addition, Fig. 3(c) shows the Nyquist plots for $CO_2$ reduction at different voltages, indicating that at low applied voltages, the process is mostly diffusion-controlled, while at higher voltages, the reaction is controlled by charge transfer resistance [27]. The impedance values (the charge transfer resistance values) are dependent on the applied voltages and are very low at higher potentials in $CO_2$ saturated solution, thus confirming higher performance and activity for $CO_2RR$. In addition to EIS, different current was applied to assess the current response and stability of the catalyst for $CO_2RR$. As can be seen in Fig. 3(d), a high and stable response was observed for the catalyst. Besides that, the total gas product was lower than 5%, which means that the catalyst is selective and stable at wide range of current densities [28, 29].

]One of the most important factors for the $CO_2ER$ is catalyst stability, in particular at high current densities (> 30 mA $cm^{-2}$). This is important because for industrialization, long-term stability is necessary. This can only be obtained if the $CO_2ER$ is doable at high stability with high applied current (means high $CO_2$ conversion rate). In this regard, we have applied two different current densities of 10 and 50 mA $cm^{-2}$ to evaluate the catalyst stability under continuous $CO_2$ electrolysis in 0.5 M $KHCO_3$. As can be seen from Fig. 4 (a and b), a stable potential record was obtained for both tested current densities. The FE result for formate for 100-h stability under 10 mA current density was almost similar with beginning and end of the test and was around 92% without significant changes in voltage responses. This shows long-time durability of prepared sample. However, as can be seen from Fig. 4b, the FE for formate at the beginning of the stability test at 50 was around 92% and remained almost unchanged after 50 h, signaling no loss of selectivity over long period of time. But after 50 h, the FE for format dropped to lower than 88% and further fallen to 55% after 68-h reaction running (Fig. S3). It is noticeable that after 65 h the FE for other gas products such as $CH_4$ and $C_2H_4$ increases which we believe that this is due to the exposer of active Cu layer. The Cu catalyst is known as the best one for ethylene and methane production from $CO_2$ electroreduction [20, 30]. As can be seen from Table 1, a brief comparison shows that we are suppressing most of the recent reported works. This further confirms our claim about working on improving catalyst stability under high current densities, because lower current seems to be doable. After 68 h continuous operation, the SEM analysis conducted to evaluate

**Fig. 4** **a** Long-time durability test at 10 mA cm⁻² for over 100 h, and **b** long-time stability result under high current density of 50 mA cm.⁻² **c** and **d** show the SEM images before and after long time CO₂ electroreduction operation
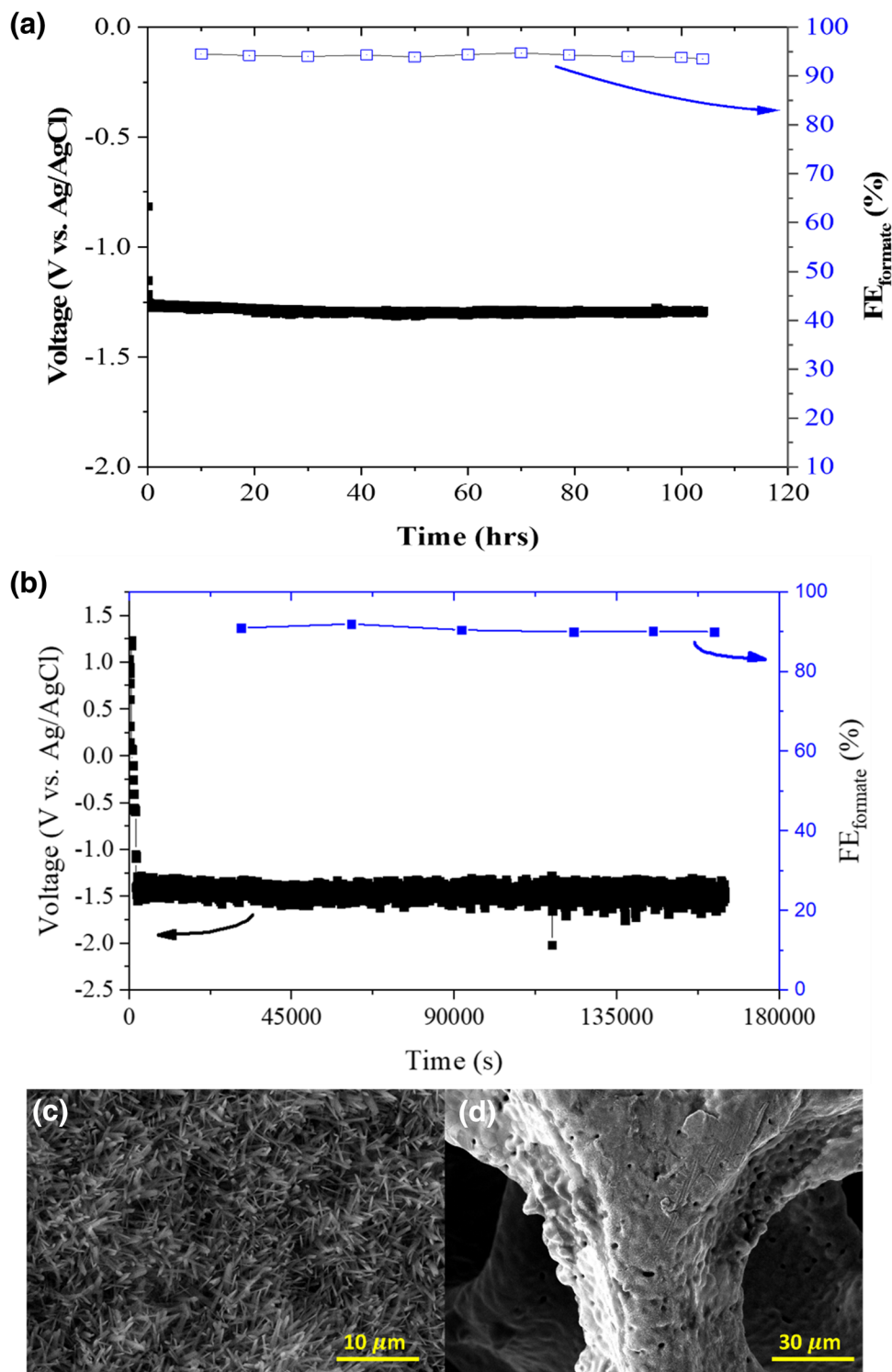


surface changes. As can be seen from Fig. S4a, the catalyst possesses an ultrafine nano-needle shape; however, after operation for 50 h, the surface of the catalyst has changed a lot (Fig. S4b). This surface reconstruction is also observed in other works; it seems that formation of $Bi_2O_2CO_3$ is possibly responsible for surface reconstruction. As discussed in

Zhang et al.'s work [31], there is possibility of formation of the Bi oxide layers during $CO_2$ conversion or exposing to air before setting up the cell. The oxidized Bi layers could react with $OH^-$ ions on surface, and form $Bi(OH)_3$. The produced $Bi(OH)_3$ is unstable under reducing condition; therefore, the formation of $Bi_2O_2CO_3$ would be facilitated as a result of

**Table 1** $CO_2RR$ performance comparison of most recently reported works

| Catalyst | Electrolyte | Formate selectivity (%) | Stability | Ref |
|---|---|---|---|---|
| $Bi_2O_3$@C | 0.5 M $KHCO_3$ | 93% | 10 h (at $-8$ mA cm$^{-2}$) | [36] |
| S-Bi-NSs | 0.5 M $KHCO_3$ | 95% | 12 h (at $-22$ mA cm$^{-2}$) | [37] |
| Bi NPs | 1 M $KHCO_3$ | 90–88% | 10 h (at $-20$ mA cm$^{-2}$) | [38] |
| S-$Bi_2O_3$-CNT | 0.5 M $KHCO_3$ | ~90% | 10 h (at approximately $-30$ mA cm$^{-2}$) | [39] |
| Bi/$Bi_2O_3$ | 0.5 M $KHCO_3$ | 70% | 10 h (at $-20$ mA cm$^{-2}$) | [40] |
| Bi/Cu foam | 0.5 M KHCO3 | >90% | ~70 h (at $-50$ mA cm$^{-2}$) | This work |
| | | | >100 h (at $-10$ mA cm$^{-2}$) | |

reacting with $CO_2$ molecules, in which the overall reaction can be summarized through the following reactions. Hence, the catalyst surface morphology will be converted over time.

$$4Bi + 3O_2 + 2H_2O \rightarrow 4BiO^+ + 4OH^-$$

$$2BiO^+ + 2CO^{2-}_3 \rightarrow Bi_2O_2CO_3$$
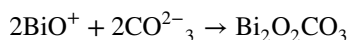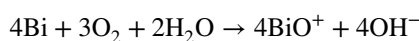
It is known that the surface reconstruction process which is the formation of inactive species such as $Bi_2O_2CO_3$ as most possible phase can decrease the overall electrocatalytic activity of the Bi electrode. Besides, after prolonged exposure to $CO_2$ electroreduction conditions, surface reconstruction of bismuth (Bi) occurs due to the migration of Bi atoms on the surface, through oxidation and leaching of Bi and redeposition on nearby surface. The formation of Bi oxide layers on the electrode surface causes the migration of Bi atoms, leading to a change in the surface structure of the Bi electrode. The migration of Bi atoms can result in the formation of Bi oxide clusters on the surface, which can act as active sites for $CO_2$ reduction reactions [32].

Also it is stated that the migration of Bi atoms on the surface of the electrode occurs due to the interaction of Bi with $CO_2$, which can result in the formation of intermediate species such as $BiCO_3$ and $BiOHCO$ [33]. These intermediate species can promote the migration of Bi atoms towards the surface, where they can form Bi oxide clusters. Additionally, the surface reconstruction of Bi can be influenced by factors such as temperature, pressure, and the composition of the electrolyte solution [34, 35].

It should be highlighted that the high performance and stability of the prepared catalyst reveal the morphological and structural benefits of Bi growth on the highly porous and conductive copper foam support; their highly accessible active sites increase the surface charge transfer phenomena. The strong contact between substrate and catalyst layer enhances the electron transfer effects, and largely available active surface area (Fig. S5) which shows that the Cu/Bi$_{48}$ possess high CV area which means that it possesses high surface area under the same condition in comparison to other conditions [41]. The support porosity due to 3D networks of

Cu foam would accelerate the diffusion of gas product during $CO_2$ reduction toward catalyst surface and detachments of the products from catalyst surface (as indicated by EIS results), which would decrease surface active site blockage and poisoning. These advantages cumulatively contributed to the high performance of the catalyst toward the $CO_2$ electroreduction process.

## Conclusion

In summary, we have successfully synthesized Bi nanostructures on Cu foam using an in situ chemical oxidation reaction and optimized the reaction time to achieve excellent performance in the $CO_2ER$ process. We hypothesize that the in situ oxidation occurs through two distinct half reactions: the slow corrosion of Cu metals from the substrate, while Bi oxide species gradually grow on the substrate, or Bi atoms absorb onto high-energy spots on the Cu foam to form Bi nanostructures. The resulting Bi structures exhibit tiny nano-needles of bismuth, with a size range of a few nanometers, offering a large accessible surface area, high porosity, and high conductivity. After extensive evaluations, we have observed that the prepared catalyst exhibits great potential in the $CO_2ER$ process, with a high FE for formate production of over 90% and excellent stability of about 50 h without losing its initial performance. Our simple yet innovative strategy resulted in a unique Bi nanostructure on Cu foam, which was optimized and characterized for $CO_2ER$, ultimately achieving high performance in the process.

**Author contribution** I.H supervised the project and contributed in experimental works. J.M.H has contributed in collecting SEM images. A.S. has contributed in preparing graphs and writing the initial draft of the paper. R.G.K has contributed in collecting XPS data and part of electrochemical data. D.O.B and N.N.G have contributed in collecting

XRD data. H.T.H has contributed in English writing and language proofing of the paper. All authors reviewed the manuscript.

## Declarations

**Ethical approval** Not applicable.

**Competing interests** The authors declare no competing interests.

## References

1. Huo H, Wang J, Fan Q, Hu Y, Yang J (2021) Cu-MOFs derived porous Cu nanoribbons with strengthened electric field for selective CO2 electroreduction to C2+ fuels. Adv Energy Mater 11(42):2102447
2. Ren B, Wen G, Gao R, Luo D, Zhang Z, Qiu W, Ma Q, Wang X, Cui Y, Ricardez-Sandoval L (2022) Nano-crumples induced Sn-Bi bimetallic interface pattern with moderate electron bank for highly efficient CO2 electroreduction. Nat Commun 13(1):1–11
3. Khiarak B, Mohammadi R, Mojaddami M, Rahmati R, Hemmati A, Simchi A (2021) Efficient electrocatalytic oxidation of water and glucose on dendritic-shaped multicomponent transition metals/spongy graphene composites. Electrochim Acta 386:138484
4. Pan H, Gong J, Zhang Y (2022) Enabling durable selectivity of CO2 electroreduction to formate achieved by a multi-layer SnOx structure. Appl Surf Sci 579:151971
5. Zhang G, Zhao Z-J, Cheng D, Li H, Yu J, Wang Q, Gao H, Guo J, Wang H, Ozin GA (2021) Efficient CO2 electroreduction on facet-selective copper films with high conversion rate. Nat Commun 12(1):1–11
6. Monteiro MC, Dattila F, Hagedoorn B, García-Muelas R, López N, Koper M (2021) Absence of CO2 electroreduction on copper, gold and silver electrodes without metal cations in solution. Nat Catal 4(8):654–662
7. Li Z, Feng Y, Li Y, Chen X, Li N, He W, Liu J (2022) Fabrication of Bi/Sn bimetallic electrode for high-performance electrochemical reduction of carbon dioxide to formate. Chem Eng J 428:130901
8. Wang X, Wang Z, de Arquer FPG, Dinh C-T, Ozden A, Li YC, Nam D-H, Li J, Liu Y-S, Wicks J (2020) Efficient electrically powered CO 2-to-ethanol via suppression of deoxygenation. Nat Energy 5(6):478–486
9. Li F, Li YC, Wang Z, Li J, Nam D-H, Lum Y, Luo M, Wang X, Ozden A, Hung S-F (2020) Cooperative CO2-to-ethanol conversion via enriched intermediates at molecule–metal catalyst interfaces. Nat Catal 3(1):75–82
10. Zhang Z, Chi M, Veith GM, Zhang P, Lutterman DA, Rosenthal J, Overbury SH, Dai S, Zhu H (2016) Rational design of Bi nanoparticles for efficient electrochemical CO2 reduction: the elucidation of size and surface condition effects. Acs Catalysis 6(9):6255–6264
11. Kibria MG, Dinh CT, Seifitokaldani A, De Luna P, Burdyny T, Quintero-Bermudez R, Ross MB, Bushuyev OS, García de Arquer FP, Yang P (2018) A surface reconstruction route to high productivity and selectivity in CO2 electroreduction toward C2+ hydrocarbons. Adv Mater 30(49):1804867
12. Xia X, Wang Y, Ruditskiy A, Xia Y (2013) Galvanic replacement: a simple and versatile route to hollow nanostructures with tunable and well-controlled properties. Adv Mater 25(44):6313–6333

13. Yao D, Tang C, Vasileff A, Zhi X, Jiao Y, Qiao SZ (2021) The controllable reconstruction of Bi-MOFs for electrochemical CO2 reduction through electrolyte and potential mediation. Angew Chem 133(33):18326–18332
14. Sheng Y, Guo Y, Yu H, Deng K, Wang Z, Li X, Wang H, Wang L, Xu Y (2023) Engineering under-coordinated active sites with tailored chemical microenvironments over mosaic bismuth nanosheets for selective CO2 electroreduction to formate. Small 2207305
15. Agapescu C, Cojocaru A, Cotarta A, Visan T (2013) Electrodeposition of bismuth, tellurium, and bismuth telluride thin films from choline chloride–oxalic acid ionic liquid. J Appl Electrochem 43:309–321
16. Jürjo S, Oll O, Paiste P, Külaviir M, Zhao J, Lust E (2022) Electrochemical co-reduction of praseodymium and bismuth from 1-butyl-1-methylpyrrolidinium bis (fluorosulfonyl) imide ionic liquid. Electrochem Commun 138:107285
17. Yang F, Liang C, Zhou W, Zhao W, Li P, Hua Z, Yu H, Chen S, Deng S, Li J, Lam YM, (2023) Oxide-derived bismuth as an efficient catalyst for electrochemical reduction of flue gas. Small 2300417
18. Jiang H, Wang L, Li Y, Gao B, Guo Y, Yan C, Zhuo M, Wang H, Zhao S (2021) High-selectivity electrochemical CO2 reduction to formate at low overpotential over Bi catalyst with hexagonal sheet structure. Appl Surf Sci 541:148577
19. Ávila-Bolívar B, Montiel V, Solla-Gullón J (2022) Electrochemical reduction of CO2 to formate on nanoparticulated Bi− Sn− Sb electrodes. ChemElectroChem 9(9):e202200272
20. García-Cruz L, Montiel V, Solla-Gullón J (2018) Shape-controlled metal nanoparticles for electrocatalytic applications. Phys Sci Rev 4(1):20170124
21. Dharmadhikari VS, Sainkar S, Badrinarayan S, Goswami A (1982) Characterisation of thin films of bismuth oxide by X-ray photoelectron spectroscopy. J Electron Spectrosc Relat Phenom 25(2):181–189
22. Ayame A, Uchida K, Iwataya M, Miyamoto M (2002) X-ray photoelectron spectroscopic study on α-and γ-bismuth molybdate surfaces exposed to hydrogen, propene and oxygen. Appl Catal A 227(1–2):7–17
23. Li L, Ma D-K, Qi F, Chen W, Huang S (2019) Bi nanoparticles/Bi2O3 nanosheets with abundant grain boundaries for efficient electrocatalytic CO2 reduction. Electrochim Acta 298:580–586
24. Kim S, Dong WJ, Gim S, Sohn W, Park JY, Yoo CJ, Jang HW, Lee J-L (2017) Shape-controlled bismuth nanoflakes as highly selective catalysts for electrochemical carbon dioxide reduction to formate. Nano Energy 39:44–52
25. Han N, Wang Y, Yang H, Deng J, Wu J, Li Y, Li Y (2018) Ultrathin bismuth nanosheets from in situ topotactic transformation for selective electrocatalytic CO2 reduction to formate. Nat Commun 9(1):1320
26. Wu D, Chen W, Wang X, Fu XZ, Luo JL (2020) Metal-support interaction enhanced electrochemical reduction of CO2 to formate between graphene and Bi nanoparticles. J CO2 Util 37:353–359
27. Khiarak B, Mojaddami M, Zamani Faradonbeh Z, Zekiy AO, Simchi A (2022) Efficient electrocatalytic overall water splitting on a copper-rich alloy: an electrochemical study. Energy Fuels 36(8):4502–4509
28. Lim HW, Park JH, Yan B, Kim JY, Lee CW (2023) Liquid-diffusion electrode with core-shell structured mixed metal oxide catalyst for near-zero polarization in chlor-alkali electrolysis. Appl Catal B 322:122095
29. Giusi D, Miceli M, Genovese C, Centi G, Perathoner S, Ampelli C (2022) In situ electrochemical characterization of CuxO-based gas-diffusion electrodes (GDEs) for CO2 electrocatalytic reduction in presence and absence of liquid electrolyte and relationship with C2+ products formation. Appl Catal B 318:121845

30. Wang Y, Liu J, Zheng G (2021) Designing copper-based catalysts for efficient carbon dioxide electroreduction. Adv Mater 33(46):2005798

31. Zhang Y, Zhang X, Ling Y, Li F, Bond AM, Zhang J (2018) Controllable synthesis of few-layer bismuth subcarbonate by electrochemical exfoliation for enhanced CO2 reduction performance. Angew Chem 130(40):13467–13471

32. Ni W, Yixiang Z, Yao Y, Wang X, Zhao R, Yang Z, Li X, Yan Y-M (2022) Surface reconstruction with a sandwich-like C/Cu/C catalyst for selective and stable CO2 electroreduction. ACS Appl Mater Interfaces 14(11):13261–13270

33. Zhang Y, Chen Y, Liu R, Wang X, Liu H, Zhu Y, Qian Q, Feng Y, Cheng M, Zhang G (2022) Oxygen vacancy stabilized Bi2O2CO3 nanosheet for CO2 electroreduction at low overpotential enables energy efficient CO-production of formate. InfoMat 5(3):e12375

34. Wang H, Tang C, Sun B, Liu J, Xia Y, Li W, Jiang C, He D, Xiao X (2022) In-situ structural evolution of Bi2O3 nanoparticle catalysts for CO2 electroreduction. Int J Extreme Manuf 4(3):035002

35. Yuan Y, Wang Q, Qiao Y, Chen X, Yang Z, Lai W, Chen T, Zhang G, Duan H, Liu M (2022) In situ structural reconstruction to generate the active sites for CO2 electroreduction on bismuth ultrathin nanosheets. Adv Energy Mater 12(29):2200970

36. Deng P, Yang F, Wang Z, Chen S, Zhou Y, Zaman S, Xia BY (2020) Metal–organic framework-derived carbon nanorods encapsulating bismuth oxides for rapid and selective CO2 electroreduction to formate. Angew Chem 132(27):10899–10905

37. Peng C-J, Zeng G, Ma D-D, Cao C, Zhou S, Wu X-T, Zhu Q-L (2021) Hydrangea-like superstructured micro/nanoreactor of topotactically converted ultrathin bismuth nanosheets for highly active CO2 electroreduction to formate. ACS Appl Mater Interfaces 13(17):20589–20597

38. Yang J, Wang X, Qu Y, Wang X, Huo H, Fan Q, Wang J, Yang LM, Wu Y (2020) Bi-based metal-organic framework derived leafy bismuth nanosheets for carbon dioxide electroreduction. Adv Energy Mater 10(36):2001709

39. Liu S-Q, Gao M-R, Feng R-F, Gong L, Zeng H, Luo J-L (2021) Electronic delocalization of bismuth oxide induced by sulfur doping for efficient CO2 electroreduction to formate. ACS Catal 11(12):7604–7612

40. Wu D, Huo G, Chen W, Fu X-Z, Luo J-L (2020) Boosting formate production at high current density from CO2 electroreduction on defect-rich hierarchical mesoporous Bi/Bi2O3 junction nanosheets. Appl Catal B 271:118957

41. Wei Q, Qin J, Jia G, Zhao Y, Guo Z, Cheng G, Ma W, Yang W, Zhang Z (2022) Dealloying-derived nanoporous bismuth for selective CO2 electroreduction to formate. J Phys Chem Letters 13(39):9058–9065